Ain Shams Engineering Journal (2015) 6, 725–733

Ain Shams University

Ain Shams Engineering Journal

www.elsevier.com/locate/asej
www.sciencedirect.com

CIVIL ENGINEERING

Reliability assessment of wall-frame structures

Reda Farag *

Department of Structures and Metallic Construction, Housing and Building Research Center, Giza 11511, Egypt

Received 2 November 2014; accepted 15 January 2015
Available online 24 March 2015

KEYWORDS

Response surface method;
Wall-frame structures;
Second order reliability method;
Reliability

Abstract Assessment of the reliability of wall-frame structures using simulation based method is often prohibited by the costly and lengthily computations. The present paper introduces a response surface based technique to quickly extract the reliability and safety information. The proposed method couples the finite element (FE) model of wall-frame structure, an improved response surface scheme and the second order reliability method (SORM). At the beginning, the large number of the random variables is reduced via preliminary sensitivity analysis. Then, the failure region is reached through a repetitive strategy integrated with recommended experimental designs. The efficiency and accuracy of the scheme are verified using Monte Carlo simulation. Moreover, both serviceability and flexural limit states are used in the verification. Tens of simulations are used instead of hundreds or thousands. The method is simple, efficient and can be easily implemented. For the considered example, the lateral load and the wall stiffness are the most important variables.

1. Introduction

Wall-frame structures are considered to be one of the most efficient and economical propositions for tall buildings. However, this system is not only highly redundant, but also has many uncertainties such as; time history loading, different material properties, complex geometrical arrangement and different sources of nonlinearities. Taking these uncertainties into account is often prohibited in the lengthily simulation based method. Fortunately, the response surface method can cut down these lengthily simulations to tens instead of hundreds or thousands. The reliability, probability of failure and other safety information can be quickly computed.

The frame-wall system is probably the most common form of reinforced concrete tall building structures. Typically, it consists of an assembly of shear walls and moment resisting frames. The shear walls are usually arranged around the elevator shafts and stair well, while the moment resisting frames are located on plan to share with the shear walls in carrying the gravity loading.

In the present paper, an improved response surface procedure is suggested, verified and implemented. In this scheme an improved response surface scheme is integrated with finite element method (FEM) method and the second order reliability method. At the beginning, a preliminary sensitivity analysis is preformed to reduce the size of the stochastic model and simplify the problem. The failure region is determined in an iterative strategy. Then the accuracy is improved without compromising the efficiency. Moreover, the most sensitive variables are determined. The results of the used response

* Tel.: +20 194342907.
E-mail address: red_bordany@yahoo.com.
Peer review under responsibility of Ain Shams University.

Production and hosting by Elsevier

http://dx.doi.org/10.1016/j.asej.2015.01.001

Nomenclature

A	effective area
b_0, b_i, b_{ii}, and b_{ij}	unknown coefficients of a polynomial to be determined
b_c, b_b	breadth of column and beam, respectively
CCD, SD	central composite design and saturated design
d_c, d_b	depth of column and beam; respectively
E	modulus of elasticity of concrete
FEM, NLFEM	finite element method and nonlinear finite element method
f_c	the compressive strength of concrete
G	the shear modulus
GA	the story-height averaged shear rigidity of the frames
$g(\mathbf{X})$	explicit expression of the limit state function
$\hat{g}(\mathbf{X})$	response surface
$g_y(\mathbf{X})$	the limit state function of drift
$\hat{g}_y(\mathbf{X})$	the response surfaces function of drift
h	the column height
H	the total height of the wall-frame structure
h_i	a chosen factor that defines the experimental/sample region
I, I_{cor}	the moment of inertia of wall and core; respectively
I_c, I_g	The moment of inertia of column and girder; respectively
I_{ic1}, I_{ic2}	the moment of inertia of internal column of frame 1 and frame 2; respectively
I_{g1}, I_{g2}	the moment of inertia of girder of frame 1 and frame 2; respectively
k	the number of random variables
L	girder span
L_w	the length of the wall cross section
m	total number of most sensitive random variables
MCS	Monte Carlo simulation
M_w	moment at the wall base
p	the numbers of coefficients necessary to define a polynomial
P	wind pressure expressed as concentrated load
P_f	the probability of failure
RSM	response surface method
SFEM	a FEM- and FORM-based reliability analysis method
SORM	second order reliability method
t_w	the thickness of shear wall
y'', y''''	second and four derivatives of lateral displacement as function in the height z
w	the wind pressure
X_{all}	the allowable drift
$\mathbf{x}_{C_1}\mathbf{x}_{C_2}$	first and second center point
$\mathbf{x}_{D_1}$	the coordinates of the checking point
X_i $(i = 1,2,\ldots,k)$	the ith random variable
X_i^C	the coordinates of the center point, i
$y(z)$	lateral drift at height z
$\alpha(X_i)$	sensitivity indexes of the variable X_i
β	β-index = reliability index
ε	pre-selected convergence criterion
$\varepsilon_{\bigcirc}$	pre-selected value
σ_{X_i}	the standard deviation of a random variable X_i

surface method (RSM) are verified using Mont Carlo simulation method (MCS).

2. Behavior of frame-shear wall structure

In a rigid frame, the accumulated horizontal shear above any story is resisted by shear in the columns of that story. The shear causes the story height columns to bend in double curvature with points of contraflexure at approximately midstory height. The moments applied to a joint from the columns above and below are resisted by the attached girders, which also bend in double curvature, with points of contraflexure at approximately midspan. The overall deflected shape of a rigid frame structure due to racking has a shear configuration with concavity upwind, a maximum inclination near the base, and a minimum inclination at the top [1].

In wall-frame structures, the flexibility of the wall/core, which behaves as a flexural cantilever is proportional to the cube of the height, while, the flexibility of the frame, which behaves as a shear cantilever is directly proportional to its height. The wall deflects in a flexural mode with concavity downwind and a maximum slope at the top, while the frame deflects in a shear mode with concavity upwind and a maximum slope at the base. The deflected shape of connected wall-frame has a flexural profile in the lower part and a shear profile in the upper part. The wall restrains the frame near the base and the frames restrain the wall at the top [1].

3. Continuum approach method

Frame-shear wall interaction has been studied in several previous works using three well known widely approaches: the continuum approach, [1], the discrete approach [2], and the successive approach [3]. This system is highly redundant. So, accurate analysis of stresses and deformations of the entire system is extremely complex. The analysis of such structures can be accurately done using 3-D FE modeling. For the sake of verification and simplicity, the continuum approaches as well as the FE methods are used.

Heidebrecht and Smith [4], Smith and Coull [1] have introduced an approximate, relatively simple mathematical solution for both static and dynamic analyses of uniform wall-frame system, the continuum approach. The wall-frame structure is considered to consist of a combination of flexural and shear vertical cantilever beams (deforming in bending and shear configuration, respectively). The method has the following assumptions:

1. The geometric properties of the wall-frame members are vertically uniform.

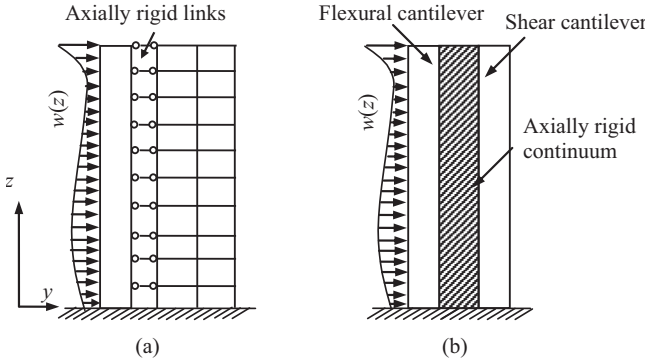

Figure 1 Planer wall-frame structure and continuum analogy.

2. The frame is represented by a continuous shear cantilever, i.e., it deflects only by reverse bending of columns and girders, and the columns are axially rigid.
3. The connecting members can be represented by rigid links which constrain both shear beam (frame) and flexural beam (wall) to have the same deflection.

The linked shear-flexure beam model, Fig. 1, has the following characteristic differential equation for the deflections:

$$y'''' - \alpha^2 y'' = w(z)EI \tag{1}$$

$$\alpha^2 = GA/EI \tag{2}$$

$$GA = \frac{12E}{h(1/G + 1/C)} \tag{3}$$

$$G = \sum I_g/L, \qquad C = \sum I_c/h \tag{4}$$

$$y = \frac{wH^4}{EI}\left\{\frac{1}{(\alpha H)^4}\left[\frac{(\alpha H \sinh \alpha H + 1)}{\cosh \alpha H}(\cosh \alpha z - 1) - \alpha H \sinh \alpha z + (\alpha H)^2\left[\frac{z}{H} - \frac{1}{2}\left(\frac{z}{H}\right)^2\right]\right]\right\} \tag{5}$$

$$M_w = wH^2\left\{\frac{1}{(\alpha H)^2}\left[\frac{(\alpha H \sinh \alpha H + 1)}{\cosh \alpha H}(\cosh \alpha z) - \alpha H \sinh \alpha z - 1\right]\right\} \tag{6}$$

where, I_g, L girder inertia and span; I_c, h column inertia and height; I core moment of inertia; E the concrete elastic modulus; w uniform wind pressure; $y(z)$ drift at height z; respectively. GA the story-height averaged shear rigidity of the frames, as though it were a shear member with an effective shear area A and a shear modulus G.

The solution of Eq. (1) leads to the drift, y Eq. (5) and the moment at wall base, M_w, Eq. (6). The method is found extensively/in detail in Smith and Coull [1].

4. Response surface methodology

The reliability analysis of complicated structural systems is accomplished either by SFEM or by RSM. SFEM evaluates the reliability by computing the gradient of the response parameters with respect to the design random variables. This evaluation requires repetitive calling of FEM. It is not practicable especially in case of nonlinear finite element (NLFEM) and time history loading. The RSM, efficiently, integrates FEM and first of second order reliability method, FORM/SORM. It advantageously represents the structures as realistic as possible by FEM/NLFEM and at the same time considers the variables uncertainties by SORM. The concept of RSM is simply to replace the response of complicated NFEM that takes lengthily computation times by an explicit approximated function. There are several types of functions to be used in approximating the structural system response; however, the best one is polynomial of low order. Therefore, a second-order polynomial without or with crossterms is usually used as

$$\hat{g}(\mathbf{X}) = b_0 + \sum_{i=1}^{k} b_i X_i + \sum_{i=1}^{k} b_{ii} X_i^2 \tag{7}$$

$$\hat{g}(\mathbf{X}) = b_0 + \sum_{i=1}^{k} b_i X_i + \sum_{i=1}^{k} b_{ii} X_i^2 + \sum_{i=1}^{k-1}\sum_{j>1}^{k} b_{ij} X_i X_j \tag{8}$$

where X_i ($i = 1,2,\ldots,k$) is the ith random variable, k is the number of random variables in the formulation and b_0, b_i, b_{ii}, and b_{ij} are unknown coefficients to be determined. The numbers of coefficients necessary to define Eqs. (7) and (8) are $p = 2k + 1$ and $(k + 1)(k + 2)/2$, respectively. The coefficients can be fully defined either by solving a set of linear equations or from regression analysis using responses at specific data points called experimental sampling points. They can be defined using the uncertainty of the random variables and a center point as follows:

$$X_i = X_i^C \pm h_i \sigma_{x_i} \quad i = 1,2,\ldots,k \tag{9}$$

where X_i^C and σ_{x_i} are the coordinates of the center point and the standard deviation of a random variable X_i, respectively, h_i is an arbitrary factor that defines the experimental region.

4.1. Experimental designs

Design of experiments is concerned with how best to locate the points in the vicinity of failure point. Saturated design (SD) and central composite design (CCD) are the two most promising designs that can be used to generate experimental sampling points around the center point. SD is less accurate but more efficient since it requires only as many sampling points as the total number of unknown coefficients to define the response surface. It can be used for both polynomials in Eq. (1) and (2), requiring $2k + 1$ and $(k + 1)(k + 2)/2$, for the two equations, respectively.

On the other hand, CCD can only be used for a polynomial with crossterms as in Eq. (2). It consists of a center point, two axial point on the axis of each random variable, at a distance $\alpha = 2^{k/4}$ from the center point and complete 2^k factorial points. CCD is more accurate but less efficient since a regression analysis needs to be carried out to evaluate the unknown coefficients in the response surface [5,6].

4.2. Failure region

The location of the center point should be at failure point, a point which is not at a hand. To determine the location of the failure point, the initial center point is taken as the mean

value point. Then, an iterative linear interpolation scheme is used as elaborated in the following.

A response surface $\hat{g}(\mathbf{X})$ can be generated explicitly in terms of the random variables X_i's by conducting deterministic finite element method analyses at all the experimental sampling points around the center point. Once an explicit expression of the limit state function $g(\mathbf{X})$ is obtained, the coordinates of the checking point $\mathbf{x}_{D_1}$ can be estimated using FORM/SORM, and all the statistical information on the X_i's. The actual response can be evaluated again at the checking point $\mathbf{x}_{D_1}$, i.e., $(g\mathbf{x}_{D_1})$ and a new center point $\mathbf{x}_{C_2}$ can be selected as:

$$\mathbf{x}_{C_2} = \mathbf{x}_{C_1} + (\mathbf{x}_{D_1} - \mathbf{x}_{C_1}) \times g(\mathbf{x}_{C_1})/(g(\mathbf{x}_{C_1}) - g(\mathbf{x}_{D_1})) \quad \text{if } g(\mathbf{x}_{D_1}) \geqslant g(\mathbf{x}_{C_1}) \tag{10}$$

$$\mathbf{x}_{C_2} = \mathbf{x}_{D_1} + (\mathbf{x}_{C_1} - \mathbf{x}_{D_1}) \times g(\mathbf{x}_{D_1})/(g(\mathbf{x}_{D_1}) - g(\mathbf{x}_{C_1})) \quad \text{if } g(\mathbf{x}_{D_1}) < g(\mathbf{x}_{C_1}) \tag{11}$$

A new center point $\mathbf{x}_{C_2}$ then can be used to develop an explicit performance function for the next iteration. This iterative strategy can be repeated until a pre-selected convergence criterion of $(\mathbf{x}_{C_{i+1}} - \mathbf{x}_{C_i})/\mathbf{x}_{C_i} \leqslant \varepsilon$ is satisfied. In the present work, ε is considered to be $|0.05|$. The iterative strategy was suggested by Bucher and Bourgund [7] and applied systematically by Rajashekhar and Ellingwood [8]. A detailed description of the RSM is available in Haldar and Mahadevan [9].

5. Efficiency and accuracy of RSM

Since the proposed algorithm is iterative and the basic SD and CCD require different amounts of computational effort, Lee and Haldar, [10] studied several schemes considering efficiency without compromising accuracy. Three schemes are of interest as follows:

1. Scheme 1: SD using quadratic polynomial without the crossterms throughout all the iterations. This scheme may be called as the known/classical response surface. It is the most efficient but least accurate in estimating the probability of failure, P_f and reliability index, β-index.

To improve the accuracy, Lee and Haldar [10] recommended the following two schemes:

2. Scheme 2: SD using quadratic polynomial without the crossterms in intermediate iterations and SD with edge points using full quadratic polynomial in the final iteration.
3. Scheme 3: SD using quadratic polynomial without the crossterms in intermediate iterations and CCD using full quadratic polynomial in the final iteration.

Considering the above three schemes, the total number of FE analyses required to generate the necessary response surface are $2k + 1$, $(k + 1)(k + 2)/2$ and $2^k + 2k + 1$, respectively, where k is the total number of random variables in the formulation. The three schemes require variant implementation effort. For example for $k = 9$, the number of required FE analyses will be 19, 55, and 531, respectively. Fig. 2 shows a diagram for the algorithm of the three schemes.

5.1. Improvement in the response surface schemes

In order to improve the efficiency, there is a need to improve the algorithm without compromising the accuracy. To meet this objective, two improvements had been developed. It is suggested here to apply these improvements to wall-frame structures under wind pressure as follows.

5.1.1. Scheme M2

To improve the efficiency of Scheme 2, it is suggested to add the crossterms (edge points), k $(k - 1)$, only of the most sensitive variables. In the last iteration, the crossterms are added only for the most sensitive random variable integrated with the corresponding edge point, to calculate the corresponding reliability index. Similarly, other less sensitive random variables can be added one by one integrated with their edge points in a sequence and the reliability index can be calculated until the changes in the reliability index become negligible. For an example, suppose the total number of basic variables is k and the total number of most sensitive random variable is m, then the total number of FE analyses required for Scheme 2 and Scheme M2 are $(k + 1)(k + 2)/2$ and $2k + 1 + m(2k - m - 1)/2$, respectively. For $k = 9$ and $m = 3$, the total number of FE analyses will be 55 and 40, respectively, for the two schemes indicating the improvement in the efficiency.

5.1.2. Scheme M3

Instead of using the full factorial plan in CCD, Myers et al. [11] recently demonstrated using half or quarter factorial plan, as shown in Fig. 2 in the coded variable space. This improved version of Scheme 2 will be denoted hereafter as Scheme M2. In Scheme M2, it is proposed that only one quarter of the factorial points corresponding to the most sensitive random variables are to be considered. If more accuracy is desired, then the analyst can use half or full factorial points. As an example for a problem with $k = 4$, the required number of sampling points will be 13, 17, and 25, for scheme quarter, half and full (CCD) factorial plan, respectively.

Based on the required accuracy, one of the above schemes can be chosen. To compare the efficiency of different schemes, the number of the required samples is plotted versus the number of variables involved in the formulation, k, as shown in Fig. 3. The curve between the points is just to show the trend. The figure shows the improvement in the efficiency, while, the accuracy is validated using two simplified examples. Three commercial codes COSMOS/M, [12] STATISTICA [13] and COMREL, [14] are used in finite element, regression and reliability analysis, respectively.

6. Statistical properties

The uncertainties in loads, material and geometric dimension can lead to failure. So these uncertainties should be taken into consideration. The wind load is assumed to follow the probability distribution of extreme value Type 1 (EV-I) distribution with coefficient of variation (COV), 37% [15]. The reinforced concrete is represented as one material (for the sake of simplicity and verification), and its strength and modulus of elasticity (f_c) and (E) are presented by lognormal distribution of 15%

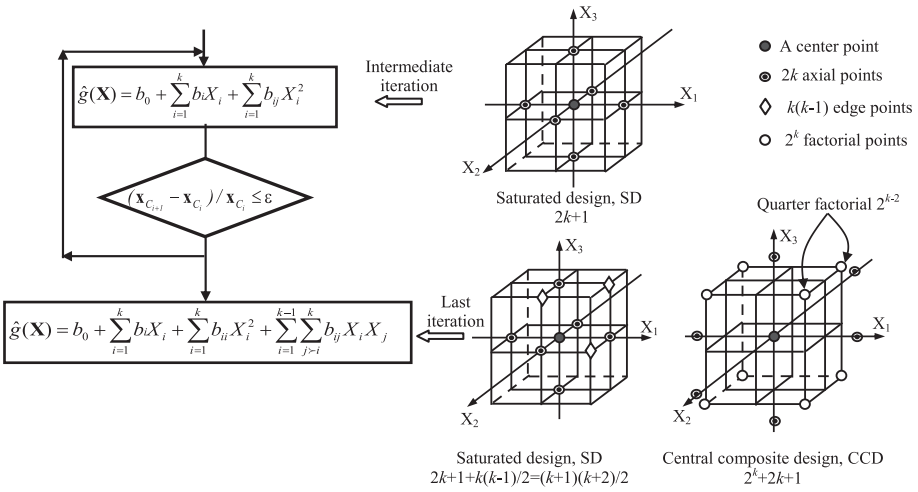

Figure 2 Algorithm of scheme 0, scheme 1 and scheme 2 (coded variable space $k = 3$).

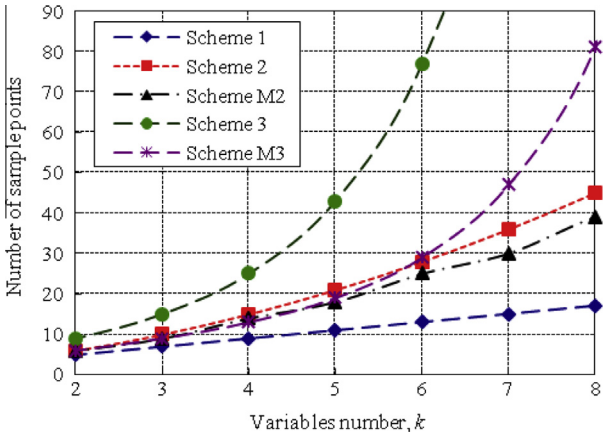

Figure 3 The efficiency of different schemes.

coefficient of variation[16]. They are related by the following equation [17]:

$$E = \begin{cases} 57,000\sqrt{f_c} & \text{psi} \\ 47,000\sqrt{f_c} & \text{N/mm}^2 \end{cases} \tag{12}$$

On the other hand, the variation in cross sectional area of columns and beams is assumed according to Mirza and MaGregor [18]. The beam breadth and depth are assumed to have standard deviation of 3/16″ (0.47625 cm) and 1/4″ (0.635 cm), respectively. The variation in the moment of inertia is assumed to be 5%.

7. Limit states

In order to avoid operational or structural failure, both serviceability and ultimate strength limit state must be far from failure, termed as SLS and ULS respectively. The wall-frame the moment at wall base and top drift limit states can be expressed as

$$g_f(\mathbf{X}) = f_c - \alpha_m \hat{g}_m(\mathbf{X}) \times y_\circ / I \tag{13}$$

$$g_y(\mathbf{X}) = X_{all} - \alpha_y \hat{g}_y(\mathbf{X}) \tag{14}$$

where $g_f(\mathbf{X})$ and $g_y(\mathbf{X})$ are the limit state function (LS) of flexural strength and drift, respectively. $\hat{g}_m(\mathbf{X})$ and $\hat{g}_y(\mathbf{X})$ are the response function of moment and drift, respectively, α_m and α_y are the model correction factors for the estimation of bending moment and drift, respectively, $y_\circ$, the distance from the neutral axis to the outer edge of the wall, I the wall moment of inertia. f_c and $X_{all,}$ are the concrete strength and the allowable drift, respectively. In the present work, $f_c = 2500\ \text{kN/m}^2$ is derived from the given $E = 2.0 \times 10^7\ \text{kN/m}^2$, in Eq. (12), while X_{all} is assumed $H/500$; where H is the structure height, respectively.

8. Numerical examples

For the sake of verification two examples are chosen from the literature. The two examples have a mathematical solution using the continuum approach method. Therefore, the verification with Monte Carlo simulation is simply done. While the first example is tall building 35 stories, the second one is a medium rise building 12 stories. Moreover, the second example is extra solved using the FE method.

8.1. Example 1: tall building 35 stories

The above outline procedure for the suggested methodology is illustrated by referring to an example of a non-twisting structure consisting of a general core and frames [1]. The plan of the structure in Fig. 4, is of a 35-story, 122.5 m-high,

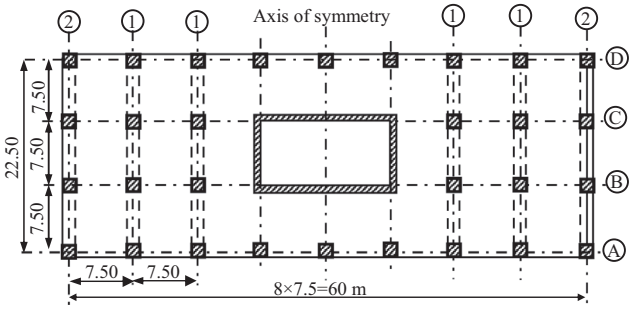

Figure 4 Plan of 35-story wall-frame – Example 1.

Table 1 Statistical characterization of random variables – Example 1.

	Random variables		Symbol	Distribution	Nominal	Mean	Bias	COV	Reference
1	Wind pressure		w	EV-I	1.5 kN/m^2	1.17	0.78	0.37	[15]
2	Concrete elastic modulus		E	LN	2.0×10^7 kN/m^2	2.0×10^7	1.00	0.15	[16]
3	Core	Inertia	I_{cor}	N	313 m^4	313	1.00	0.05[a]	
4	Frame 1	Interior column	I_{ic1}	N	0.083 m^4	0.083	1.00	0.05[a]	
5		Exterior column	I_{ec1}	N	0.050 m^4	0.050	1.00	0.0 [a]	
6		Girder	I_{g1}	N	0.011 m^4	0.011	1.00	0.05[a]	
7	Frame 2	Interior column	I_{ic2}	N	0.050 m^4	0.050	1.00	0.05[a]	
8		Exterior column	I_{ec2}	N	0.034 m^4	0.034	1.00	0.05[a]	
9		Girder	I_{g2}	N	0.005 m^4	0.005	1.00	0.05[a]	
10	Concrete strength		f_c	LN	2000 kN/m^2	2000	1.00	0.15	[16]

[a] Data are not available. Assumed parameters are based on engineering judgment.

wall-frame structure. The horizontal resistance to wind acting on its long side is provided by six rigid frame bents and a central core. Given that the core inertia is 313 m^4 and the concrete elastic modulus is 2.0×10^7 kN/m^2, it is required to find the reliability against a wind loading 1.5 kN/m^2. The inertia of frame columns and girders is given in Table 1.

The lateral drift and the moment at the wall base are expressed based on the continuum approach as in Eqs. (5) and (6), respectively.

8.1.1. Drift limit state

First, the verification is performed for the drift LS as follows.

Using Eq. (5) and Monte Carlo simulation (MCS), the probability of failure and the reliability index are found to be $P_f\text{-}MCS = 5.73\times10^{-2}$ and $\beta\text{-}MCS = 1.578$, respectively. Re-computing these values again using SORM, very close values are obtained as listed in Table 2.

Then, the proposed algorithm is started by a preliminary sensitivity analysis using first order polynomial (the same as Eq. (7), but without the quadratic terms). The variables of low sensitivities less than selected value ($<\varepsilon_{\bigcirc}$) can be considered as constant values. In this example, $\varepsilon_{\bigcirc}$ is assumed 3%. As a result, the 9-variable problem is reduced to 4-variable problem. The four variables are: the wind pressure (w), the elastic modulus (E), the core moment of inertia (I_{cor}) and the girder inertia of the interior frame 1 (I_{g1}), sensitive's: −0.972, 0.229, 0.037 and 0.033, respectively. Then, the analysis is continued by a quadratic polynomial function, Eq. (7). Following the iterative scheme, the drift is represented using scheme 1 and yields the following limit state function:

$$\begin{aligned}\hat{g}_y(\mathbf{X}) &= X_{all} - \hat{g}_y(\mathbf{X}) = H/500 \\ &- \Big[0.822 + 0.129\times w - 0.404\times E\times10^{-7} - 7.268 \\ &\times10^{-4}\times I_{cor} - 18.174\times I_{g1} + 5.200\times10^{-13}\times w^2 + 7.220 \\ &\times10^{-9}\times E^2 + 5.826\times10^{-7}\times I_{cor}^2 - 410.227\times I_{g1}^2\Big] \qquad (14)\end{aligned}$$

The β-index is found to be 1.513. The accuracy of this value can be improved by adding the crossterms of the most important variable; w using 3 more function calls (scheme M2-1). The β-indexes for scheme 1 and scheme M2-1 are 1.513 and 1.564 (4.1% and 0.9% less than β-MCS) using 15 and 12 function calls, respectively, where scheme M2-1 terms to scheme M2 when only the most important random variable is added. If more accuracy than scheme M2-1 is desired, the crossterms of the second important variable E can be added using 2 more function calls (scheme M2-2) and so on.

On the other hand, the β-indexes for scheme M3 and scheme 3 (with quarter, half and full factorial points) are 1.524, 1.539 and 1.570 (3.4%, 2.5% and 0.5% less than β-MCS) using 13, 17 and 25 function calls, respectively.

8.1.2. Strength limit state

Substituting the given value of for $E = 2.0\times10^7$ = kN/m^2, the allowable concrete strength f_c = 2000 kN/m^2.

Table 2 Results of reliability analysis (drift limit state) – Example 1.

			Variables sensitivities, $\alpha(X_i)$				β	P_f	No. of calls
			w	E_c	I_{cor}	I_{g1}			
	(i) Explicit limit state								
1	Monte Carlo – 9 variables						1.578	5.73×10^{-2}	10^5
2	SORM – 9 variables		−0.921	−0.381	−0.059	0.053	1.574	5.77×10^{-2}	1
	(ii) Response surface								
3	First order polynomial		−0.972	0.229	0.037	0.033	1.676	4.68×10^{-2}	19
4	Scheme 1		−0.907	−0.414	−0.061	0.054	1.513	6.51×10^{-2}	9
5	Scheme M2-1	w	−0.917	0.392	−0.058	0.051	1.564	5.89×10^{-2}	12
	Scheme M2-2	w, E_c	−0.916	0.393	−0.060	0.053	1.566	5.87×10^{-2}	14
	Scheme M2-3	w, E_c, I_{cor}	−0.916	0.393	−0.060	0.053	1.564	5.89×10^{-2}	15
6	Scheme 2		−0.916	0.393	−0.060	0.053	1.564	5.89×10^{-2}	15
7	Scheme M3	Quarter	−0.899	0.432	−0.056	0.052	1.524	6.37×10^{-2}	12
		Half	−0.901	0.427	−0.059	0.053	1.539	6.19×10^{-2}	14
	Scheme 3	Full	−0.916	0.394	−0.059	0.052	1.570	5.82×10^{-2}	15

Following the same procedure as in drift limit state, the preliminary reliability analysis reduces the 9-variables to three variables: wind pressure (w), the core inertia (I_{cor}) and the girder inertia of the interior frame (I_{g1}). At the end of the iterative strategy, scheme 1 yields the following limit state function:

$$g_f(\mathbf{X}) = f_c - \alpha_m \hat{g}_m(\mathbf{X}) \times y_\circ / I_{cor} = f_c - \left[-279,763.885 + 286,649.942 \times w + 2255.701 \times I_{cor} - 19,853,107.714 \times I_{g1} - 858.740 \times w^2 - 2.171 \times I_{cor}^2 - 426,003.962 \times I_{g1}^2\right] \quad (15)$$

The β-index is found to be 3.093, as shown in Table 3. The accuracy of this value can be improved by adding the crossterms of the most important variable; w using 2 more function calls (scheme M2-1). The β-indexes for scheme 1 and scheme M2-1 are 3.093 and 3.094 (0.45% and 0.49% more than β-MCS) using 15 and 12 function calls, respectively. If more accuracy than scheme M2-1 is desired, the crossterms of the second important variable I_{cor} can be added using 1 more function call (scheme M2-2). On the other hand, the β-indexes for CCD based schemes of quarter, half and full factorial points are 3.093, 3.093 and 3.093 (0.45%, more than β-MCS) using 13, 17 and 25 function calls, respectively.

The most important random variables are the wind pressure (w), the concrete strength (f_c), the core inertia (I_{cor}) and the girder inertia of the interior frame (I_{g1}); respectively.

8.2. Example 2

The floor plan of anther building is shown in Fig. 5. The building comprises two shear walls and four peripheral frames [19]. The thickness of the walls is 15 cm while the dimensions of the columns and beams are 40×60 cm^2 and 20×60 cm^2, respectively. The story height is 3.00 m while the Young's modulus of elasticity of concrete is taken as 20×10^6 kN/m^2. A uniformly distributed wind load of 10 kN per floor is assumed, acting on the structure in the positive x-direction. The given data as well as their statistical properties are listed in Table 4.

As in the previous example, using Eq. (5) and Monte Carlo simulation (MCS), the probability of failure and the reliability index of drift limit state are found to be P_f-$MCS = 4.60 \times 10^{-4}$ and β-$MCS = 3.314$, respectively. Re-computing both of them

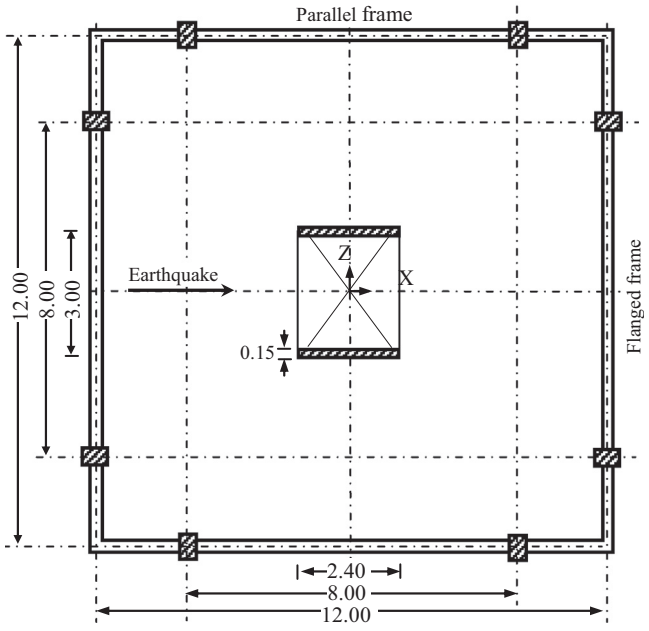

Figure 5 Structural plan of example 2.

again using SORM, very close values are obtained as listed in Table 5.

For the sake of further verification, a planer FE model is set up as shown in Fig. 6. Performing 17 FE runs at sample points according to equation (9), a preliminary analysis reduces the problem to 4-variable problem: the wind load (P), the elastic modulus (E), the beam depth and breadth (d_b and b_b). Then, following the iterative scheme, the drift is represented using scheme 1 and yields the following limit state function:

$$\hat{g}_y(\mathbf{X}) = X_{all} - \hat{g}_y(\mathbf{X}) = H/500 - \left[0.551 + 2.249 \times 10^{-3} \times P - 0.120 \times 10^{-7} \times E - 0.864 \times d_b - 0.580 \times b_b + 0.0 \times p^2 + 21.678 \times 10^{-10} \times E^2 + 0.538 \times d_b^2 + 0.904 \times b_b^2\right] \quad (16)$$

The reliability indices of the drift limit state for scheme 1 and scheme M2-1, scheme M2-2 and scheme M2-3 are 3.230, 3.338, 3.338 and 3.330 respectively. These values are −2.53%, 0.72%, 0.72% and 0.48% different from β-MCS.

Table 3 Results of reliability analysis (flexural strength limit state) – Example 1.

			Variables sensitivities, $\alpha(X_i)$				β	Error (%)	P_f	No. of calls
			f_c	w	I_{cor}	I_{g1}				
	(i) Explicit limit state									
1	Monte Carlo – 9 variables						3.079		10.4×10^{-4}	10^5
2	SORM – 9 variables		0.390	−0.915	0.096	0.028	3.091	0.39	9.97×10^{-4}	1
	(ii) Response surface									
3	First order polynomial		0.389	−0.914	0.119	0.011	3.085	0.19	10.2×10^{-4}	19
4	Scheme 1		0.391	−0.916	0.089	0.034	3.093	0.45	9.91×10^{-4}	7
5	Scheme M2-1	w	0.389	−0.916	0.096	0.028	3.094	0.49	9.89×10^{-4}	9
	Scheme M2-2	w, I_{cor}	0.389	−0.916	0.096	0.028	3.094	0.49	9.89×10^{-4}	10
6	Scheme 2		0.389	−0.916	0.096	0.028	3.094	0.49	9.89×10^{-4}	10
7	Scheme M3	Quarter	0.389	−0.916	0.096	0.028	3.093	0.45	9.91×10^{-4}	9
		Half	0.389	−0.916	0.096	0.028	3.093	0.45	9.91×10^{-4}	11
	Scheme 3	Full	0.389	−0.916	0.096	0.028	3.093	0.45	9.92×10^{-4}	15

Table 4 Statistical characterization of random variables – Example 2.

	Random variables		Symbol	Distribution	Nominal	Mean	Bias	COV	Reference
1	Lateral load		P	EV-I	12.82 kN	10	0.78	0.37	[15]
2	Concrete elastic modulus		E	LN	20×10^6 kN/m^2	20×10^6	1.00	0.15	[16]
3	Shear wall	Thickness	t_w	LN	0.15 m	0.15	1.00	0.042	[18]
4		Width	L_w	LN	2.40 m	2.40	1.00	0.003	[18]
5	Column	Breadth	b_c	N	0.40 m	0.40	1.00	0.016	[18]
6		Depth	d_c	N	0.60 m	0.60	1.00	0.011	[18]
7	Beam	Breadth	b_b	N	0.20 m	0.20	1.00	0.024	[18]
8		Depth	d_b	N	0.60 m	0.60	1.00	0.011	[18]

Table 5 Results of reliability analysis (drift limit state) – Example 2.

			Variables sensitivities, $\alpha(X_i)$				β	Error (%)	P_f	No. of calls
			P	E_c	d_b	b_b				
	(i) Explicit limit state									
1	Monte Carlo						3.314		4.60×10^{-4}	10^5
2	SORM		−0.915	0.397	0.054	0.039	3.357	1.30	3.94×10^{-4}	1
	(ii) Response surface									
	First order polynomial		−0.992	0.125	0.018	0.013	3.675	10.89	1.19×10^{-4}	17
	Scheme 1		−0.853	0.516	0.061	0.045	3.230	−2.53	6.19×10^{-4}	9
3	Scheme M2-1	P	−0.907	0.416	0.047	0.034	3.338	0.72	4.21×10^{-4}	12
	Scheme M2-2	P, E	−0.907	0.417	0.054	0.039	3.338	0.72	4.23×10^{-4}	14
	Scheme M2-3	P, E, db	−0.907	0.416	0.054	0.039	3.330	0.48	4.34×10^{-4}	15
4	Scheme 2		−0.907	0.416	0.054	0.039	3.330	0.48	4.34×10^{-4}	15
5	Scheme 3	Quarter	−0.846	0.532	0.037	0.021	3.214	−3.02	6.53×10^{-4}	11
		Half	−0.849	0.524	0.055	0.040	3.217	−2.93	6.48×10^{-4}	15
		Full	−0.909	0.410	0.053	0.039	3.346	0.97	4.11×10^{-4}	25

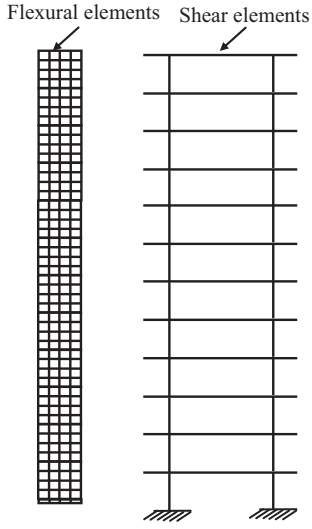

Figure 6 Planer wall-frame FE model – Example 2.

On the other hand, the reliability indices of the strength limit state using one of central composite based designs quarter, half or full, are 3.214, 3.217 and 3.346; respectively. These values are −3.02%, −2.93% and 0.97% different from β-*MCS*.

The probability of failures resulted from the different schemes is listed in Table 5. The most important random variables are the wind load (P), the elastic modulus (E), the beam depth and breadth (db and bb); respectively.

9. Discussion

The efficiency of the response surface scheme is improved and validated. In the drift limit state, the most important variables are the wind load and the elastic modulus, while for the strength limit state, the important variables are the wind load and the concrete strength.

In the case of non-uniform or non-symmetric wall-frame structures, the analyst cannot apply the continuum analogy. He has only the FE model at the hand. Following the suggested procedure, the safety information can be easily extracted. Furthermore, the level of the accuracy can be selected. In other words, if the analyst manipulates a temporary structure, scheme 1 of low accuracy is sufficient. However, other more accurate schemes can be used in cases of tall wall-frame of special importance which may be built for vital structures.

10. Conclusion

In the present paper, an efficient and accurate response surface algorithm is suggested to evaluate the reliability of wall-frame structures. It is suggested to improve the computational efficiency of the response surface method. Uncertainties in load, material and geometrical details are incorporated. The method integrates the concept of response surface method, FE method and the second order reliability method. The sensitivity analysis is used to improve the efficiency further.

With the help of two literature examples, it is elaborated that the proposed algorithm can be used in estimating the safety. The efficiency and accuracy of the proposed schemes are demonstrated. The improvements are effective and can be used to estimate the safety of wall-frame structure. Furthermore, the safety corresponding to operational and structural limit states of full size example is investigated. It has been found that the most influential variables are wind loading and the concrete elastic modulus for drift limit state, while the most sensitive variables are the wind load and the concrete strength for the moment at the wall base.

References

[1] Smith BS, Coull A. Tall building structures: analysis and design. Wiley; 1991.

[2] Coull A, Abdul Wahab A. Lateral load distribution in asymmetrical tall building structures. J Struct Eng 1993;119(4):1032–47.

[3] Pala S, Özmen G. Lateral load analysis of multi-storey structures considering axial deformations. Comput Struct 1990;34(4):577–83.

[4] Heidebrecht A, Smith B. Approximate analysis of tall wall-frame structures. J Struct Eng 1973;99(2):255–82.

[5] Box GEP, Hunter WG, Hunter JS. Statistics for experimenters: an introduction to design, data analysis, and model building. Wiley; 1978.

[6] Khuri AI, Cornell JA. Response surfaces: designs and analyses. 2nd ed. Taylor & Francis; 1996.

[7] Bucher CG, Bourgund U. A fast and efficient response surface approach for structural reliability problems. Struct Saf 1990;7(1):57–66.

[8] Rajashekhar MR, Ellingwood BR. A new look at the response surface approach for reliability analysis. Struct Saf 1993;12(3):205–20.

[9] Haldar A, Mahadevan S. Reliability assessment using stochastic finite element analysis. Wiley; 2000.

[10] Lee S, Haldar A. Reliability of frame and shear wall structural systems. II: Dynamic loading. J Struct Eng 2003;129(2):233–40.

[11] Myers RH, Montgomery DC, Anderson-Cook CM. Response surface methodology: process and product optimization using designed experiments. Wiley; 2009.

[12] Corporation, S.r.a.a. Cosmos/m 2.6. 2000. <http://www.cosmosm.com>.

[13] StatSoft. Statistica. 1984. <http://www.statsoft.com>.

[14] RCP. Comrel 6.10. 1987–1997. <http://www.strurel.de>.

[15] Ellingwood B. Development of a probability based load criterion for american national standard a58: building code requirements for minimum design loads in buildings and other structures. U.S. Department of Commerce, National Bureau of Standards; 1980.

[16] Joint Committed of Structural Safety. Probabilistic model code: Part 3: Material properties, concrete properties; 2000.

[17] Ameur-Moussa R, Buyukozturk O. A bounding surface model for concrete. Nucl Eng Des 1990;121(1):113–25.

[18] Mirza S, MacGregor J. Variations in dimensions of reinforced concrete members. J Struct Eng 1979;105(4):751–66.

[19] Swaddiwudhipong S, Piriyakoontorn S, Lim Y-B, Lee S-L. Analysis of tall buildings considering the effect of axial deformation by the Galerkin method. Comput Struct 1989;32(6):1363–9.

Reda Farag is an assistant professor in HBRC. He got his PhD from Ain Shams University.